The role of added polymer in dilute lamellar surfactant phases

J. T. Brooks and M. E. Cates[a)]
Theory of Condensed Matter, Cavendish Laboratory, Madingley Road, Cambridge CB3 0HE, United Kingdom

(Received 3 May 1993; accepted 14 June 1993)

We study theoretically the effect of adding polymer to the dilute lamellar phase of surfactant solutions. The polymer, assumed semidilute and in a good solvent, is taken to have a repulsive or attractive interaction with surfactant bilayers, but has no other effect on their properties. Such polymers can mediate an attractive or repulsive interaction between bilayers which we combine with pre-existing interactions (the Helfrich repulsion, van der Waals, and hydration) using a simple additive model. The polymeric contribution to the free energy is estimated using a blob model (for nonadsorbing chains) and the Cahn–de Gennes scaling functional (for adsorbing chains). Phase diagrams for the system are obtained under various conditions. For a lamellar phase which is bound (i.e., which cannot be indefinitely diluted) as a result of van der Waals forces, nonadsorbing polymer is completely expelled as a semidilute solution, leading to a compression of the lamellar stack. Adsorbing polymer can enter the phase, also tending to cause a slight reduction in the maximum layer spacing. For an unbound lamellar phase controlled by Helfrich forces, nonadsorbing polymer is expelled if the bilayers are stiff, but for flexible enough layers, a significant amount of polymer can be solubilized. At too high a volume fraction of polymer, part of the polymer is expelled as a solution, whereas at high surfactant fractions, a phase separation arises between two lamellar phases (one containing polymer, the other not). For the case of adsorbing chains, small amounts of added polymer cause the system to become bound with expulsion of excess solvent. For large amounts of added polymer, the unbound behavior is recovered, whereas for intermediate polymer content, phase equilibria involve either two lamellar phases (each containing polymer), or one such phase coexisting with a polymer solution.

I. INTRODUCTION

Surfactant systems are of great interest in the realms of physics, chemistry, and biological science, and are widely used in industry as emulsifiers, detergents, and suspending agents. Many industrial products use mixtures of both surfactant and polymer molecules; the presence of polymers modifies the properties of the system, e.g., to give a desired rheological response (lubricants), or to stabilize a particular state of surfactant organization (fabric conditioners, etc.).

From a theoretical point of view, the surfactant lamellar mesophase presents a convenient system to consider the effect of added polymer; the nature of the lamellar phase itself is now well understood. Little experimental work has so far been published on the addition of polymers to the lamellar phase, although we are aware of one study[1] of highly concentrated lamellar phases (surfactant volume fractions of the order of 70%), where the polymer combines in a nontrivial way with the surfactant bilayers. In this paper, however, we are mainly interested in the role of added homopolymer in the dilute lamellar phase.

For simplicity, we restrict our discussion to uncharged systems and suppose that the bilayers retain their integrity upon addition of polymer to the solvent. In this case, there is obviously a close link between the properties of a polymer-containing lamellar phase (when this is stable) and the polymer-mediated forces between surfaces. Indeed, one can think of a lamellar phase containing polymer as a naturally occurring "surface force machine." The *bulk* thermodynamics of the phase (osmotic pressure, etc.) are intimately related to the *surface forces* between polymer-bearing sheets and could under favorable conditions be used to probe these forces.

Before outlining our approach, let us briefly review the nature of the lamellar mesophase of surfactants. The lamellar phase, a stack of bilayers with one-dimensional long-range order, can be either "bound" or "unbound," depending on the nature of the interlamellar interactions. The bound state cannot be diluted indefinitely, but will expel excess solvent beyond a certain maximal dilution. This is not true of the unbound state. The transition between these two states is referred to as the unbinding transition and depends delicately on the membrane–membrane interactions. In recent theoretical work, Leibler and Lipowsky[2,3] have argued, using renormalization group calculations, that the system can undergo a continuous transition from a bound state to an unbound state when an intensive parameter, e.g., the Hamaker constant W, is varied. In the presence of an attractive van der Waals interaction, the transition occurs at a nonzero value for W, which balances a tendency toward unbound behavior provided by the Helfrich steric repulsion. More recently, a mean-field picture of the transition was proposed by Milner and Roux.[4] This

a)To whom correspondence should be addressed.

 0021-9606/93/99(7)/5467/14/$6.00

model treats the direct interactions within a perturbative framework, recovering all the main features of the transition described by the renormalization group methods of Leibler and Lipowsky. To date there has been no direct experimental evidence to prove or disprove the second order nature of the unbinding transition.

A far simpler "classical" model has been proposed, e.g., by Wennerstrom,[5] in which the Helfrich interaction energy, direct membrane interactions, and a chemical potential term are added together. The results indicate a first order transition between bilayers bound at a distance of order the bilayer thickness and essentially unbound bilayers. As emphasized by Leibler and Lipowsky,[2] this cannot be an appropriate model for critical (i.e., continuous) unbinding; it is contradictory to assume that the bilayers maintain a well-defined separation (to estimate the direct interactions), and at the same time, that the Helfrich interaction (caused by departures from flatness) is responsible for the repulsion between bilayers. However, despite being unable to predict the correct order of the transition, this "additive" model enables the phase equilibria of the system to be simply found and should give reasonable results if parameter values far from critical are adopted.

In summary, the additive model provides a convenient initial framework in which to discuss the phase equilibria of the lamellar system (provided we are not too close to critical unbinding), and we now propose to incorporate the effects of added homopolymer within the same scheme. We can consider that polymer sequestered in the interlamellar regions will have two effects—renormalization of the elastic moduli (and hence of the Helfrich interaction) and the production of a direct polymer-mediated interlamellar interaction. Obviously, these two effects are coupled, but at the level of the additive approach, we consider them as independent. In previous work,[6,7] we demonstrated that the shift in the elastic moduli of a surfactant bilayer due to the addition of adsorbing homopolymer is typically small compared to the bare surfactant elastic moduli (except in the regime of very strong adsorption). A similar investigation using nonadsorbing homopolymer produces results which are also negligibly small.[8] Thus under most conditions of interest, the renormalization of the Helfrich interaction will be relatively weak, and in what follows we neglect this effect, considering only the polymer-mediated interlamellar interaction between nominally flat sheets.

The remainder of this paper is organized as follows: In Sec. II, we consider the phase equilibria of the mixed polymer–lamellar system for the case of nonadsorbing polymer. In Secs. II A and II B, we formulate the polymer free energy and go on in Secs. II C and II D to consider the perturbing effect of polymer on unbound and bound lamellar surfactant phases, respectively. In Sec. III, we repeat the procedure using adsorbing polymer before summarizing and discussing our results in Sec. IV. We restrict our analysis throughout to the case where the added polymer is semidilute and governed by good solvent conditions.

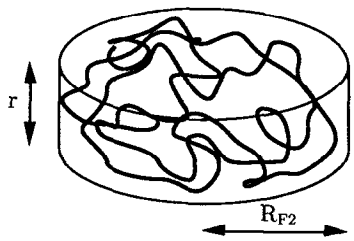

FIG. 1. Pancake correlation blob of thickness r and radius R_{F2}.

II. NONADSORBING POLYMER

A. Statistics of confined nonadsorbing polymer chains

The statistics of nonadsorbing polymer solutions trapped in small pores was considered by Daoud and de Gennes.[9] The problem studied by these authors is very similar to our own; we adopt their approach. Consider first a single chain in a bulk solvent. The size of the chain is R_{F3} (where F stands for Flory and 3 for three dimensional)[10]

$$R_{F3} \simeq a N^{3/5}, \tag{1}$$

where a is a monomeric length and N the degree of polymerization. Now let us place the chain inside an interlamellar region, where we approximate the bilayers as being flat and the average interlamellar spacing is given by r. If $r \gg R_{F3}$, no change in shape is expected, whereas if $r < R_{F3}$, significant squeezing of the chain must take place; a spherical coil becomes a flat "pancake" with thickness r and radius R_{F2} (see Fig. 1). By invoking the Flory argument,[11] the two-dimensional radius R_{F2} must be proportional to $N^{3/4}$. A straightforward scaling argument[10] for R_{F2} yields

$$R_{F2} \simeq a N^{3/4} \left(\frac{a}{r}\right)^{1/4}. \tag{2}$$

The above refers to the behavior of a single chain; clearly this will change when different chains come into contact. We now introduce an overlap concentration $c^*(x)$, where $x = R_{F3}/r$, with the following properties:

(1) For $x \ll 1$, $c^* = c_3^*$ is the three-dimensional overlap concentration[10]

$$c_3^* \simeq \frac{N}{R_{F3}^3} \simeq a^{-3} N^{-4/5}. \tag{3}$$

(2) For $x \gg 1$, c^* corresponds to having N monomers in a volume of $r R_{F2}^2$,

$$c_2^*(x) \simeq \frac{N}{r R_{F2}^2} \simeq c_3^* x^{1/2}. \tag{4}$$

In what follows, we assume $c \gg c^*$, i.e., we restrict ourselves to the semidilute regime and denote the average monomer volume fraction *in the solvent* as $\bar{\phi}$. We can also define $\xi_3(\bar{\phi})$, the correlation length for a bulk solution of concentration $\bar{\phi}$, which may be interpreted using the concept of "blobs."[10] Each chain is regarded as a sequence of blobs having $g = (\xi_3/a)^{5/3}$ monomers and diameter ξ_3. Inside

each blob, excluded-volume effects are important, but different blobs are essentially uncorrelated; the chains are ideal at large length scales. As usual, ξ_3 obeys

$$\xi_3 \simeq a\bar{\phi}^{-3/4}. \tag{5}$$

In terms of the correlation length, we can envisage two different regimes. If $r \gg \xi_3$, the polymer solution is essentially a bulk solution with depletion regions of order ξ_3 near each surface;[12] the chains are governed by the usual three-dimensional statistics. For $r \ll \xi_3$, the statistics must be strongly two dimensional. With reference to our previous discussion of a confined single chain, we can imagine the solution to be composed of pancake-shaped blobs of width r and radius ξ_2, where ξ_2 is a correlation length in the interlamellar plane. This correlation length, as in the case of a bulk solution, must depend on $\bar{\phi}$, but be independent of the degree of polymerization N. In an analagous manner to the three-dimensional case, we can write

$$\xi_2 \simeq R_{F2}\left(\frac{\bar{\phi}}{\bar{\phi}_2^*}\right)^n. \tag{6}$$

Demanding that ξ_2 is independent of N sets the exponent n to be $n=-3/2$, and thus

$$\xi_2 \simeq \left(\frac{a^2}{r}\right)\bar{\phi}^{-3/2}. \tag{7}$$

B. Polymer free energy

We now consider the polymer free energy within the polymer–lamellar system. Units are chosen with $k_B=1$. We focus on the two limiting cases just considered.

(1) $r \gg \xi_3$. In this limit, the surfaces can be viewed as independent. The corresponding free energy then consists of a "bulk" contribution and a term associated with the depletion of polymer near each surface. The free energy of depletion per unit area (of a one-sided surface) is of order of the work done against the bulk osmotic pressure Π to remove a slab of solution of width ξ_3 (Ref. 12)

$$\frac{F_{\text{dep}}}{A} \sim \Pi\xi_3. \tag{8}$$

Combining this with the usual bulk free energy contribution $\sim T/\xi_3^3$ gives the total free energy per unit area of bilayer as

$$\frac{F}{A} = \frac{\beta T}{a^3}\bar{\phi}^{9/4}r + 2\frac{\rho T}{a^2}\bar{\phi}^{3/2}, \tag{9}$$

where β and ρ are universal prefactors discussed below. (The factor of 2 arises because we have a two-sided problem.)

(2) $r \ll \xi_3$. In this limit, the chains are strongly compressed and, as discussed in Sec. II A, can be regarded as pancakes of width r and radius ξ_2. The free energy now consists of the work required to compress a spherical blob into a pancake (entropic confinement term) and the work involved in bringing pancake-shaped blobs into contact (osmotic pressure term). To determine the scaling of these terms, we count the correlation blobs and ascribe the thermal energy T to each. Let us first consider the entropic confinement contribution. Inside each pancake blob (of size ξ_2) a chain follows an excluded random walk in two dimensions, where the fundamental unit is a spherical r blob of diameter r (see Fig. 2). The number of r blobs in each pancake blob is given by the Flory argument as $(\xi_2/r)^{4/3}$ (Ref. 9) and the number of r blobs per unit area is $1/\xi_2^2 \cdot (\xi_2/r)^{4/3}$. The entropic confinement contribution is therefore

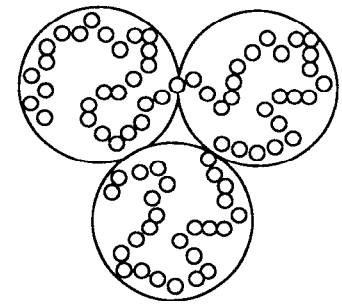

FIG. 2. Plan view of the confined polymer chains. Inside each large pancake correlation blob (of size ξ_2) a chain follows an excluded random walk in two dimensions, where the blobs are spherical with diameter r.

$$\frac{F_{\text{conf}}}{A} \sim \frac{T}{\xi_2^2}\left(\frac{\xi_2}{r}\right)^{4/3}. \tag{10}$$

The work required to bring the pancake blobs into contact against the two-dimensional osmotic pressure is T per pancake blob of size ξ_2

$$\frac{F_{\text{osmo}}}{A} \sim \frac{T}{\xi_2^2}. \tag{11}$$

Finally, rewriting ξ_2 in terms of $\bar{\phi}$, according to Eq. (7), gives the free energy per unit area in the $r \ll \xi_3$ limit as

$$\frac{F}{A} = \frac{\delta T}{a^2}\left(\frac{a}{r}\right)^{2/3}\bar{\phi} + \frac{\eta T}{a^2}\left(\frac{r}{a}\right)^2\bar{\phi}^3, \tag{12}$$

where δ and η are unknown numerical prefactors (discussed below).

To proceed further, we must now write our free energy expressions in terms of the fundamental composition variables, namely, the volume fraction of polymer Φ and volume fraction of surfactant ψ. The volume fraction of surfactant ψ is related by geometry to the mean interlamellar spacing r,[13]

$$\frac{r}{L} = \frac{(1-\psi)}{\psi}, \tag{13}$$

where L is the bilayer thickness. Likewise, the volume fraction of polymer *in the system* Φ is related to the average volume fraction of polymer *in the solvent* by

$$\Phi = \bar{\phi}(1-\psi). \tag{14}$$

Rewriting the polymer free energy per unit area [Eqs. (9) and (12)] in terms of Φ and ψ according to Eqs. (13) and (14) gives

$$\frac{F_{\text{poly}}}{A}=\left[\frac{\beta T}{a^2}\left(\frac{L}{a}\right)\frac{\Phi^{9/4}}{\psi(1-\psi)^{5/4}}+2\frac{\rho T}{a^2}\frac{\Phi^{3/2}}{(1-\psi)^{3/2}}\right],$$

for $r\gg\xi_3$,

$$=\left[\frac{\delta T}{a^2}\left(\frac{a}{L}\right)^{2/3}\frac{\psi^{2/3}\Phi}{(1-\psi)^{5/3}}+\frac{\eta T}{a^2}\left(\frac{L}{a}\right)^2\frac{\Phi^3}{\psi^2(1-\psi)}\right],$$

for $r\ll\xi_3$. (15)

To address the phase equilibria of the mixed polymer–lamellar system, we need an estimate for the polymer free energy that is continuous with respect to the ratio r/ξ_3, i.e., the composition variables Φ and ψ. To avoid spurious phase transitions, we also require continuity in the first derivatives of the polymer free energy (with respect to the composition variables Φ and ψ). We therefore demand that the two limiting forms in Eq. (15) match smoothly [i.e., F_{poly}/A, $\partial(F_{\text{poly}}/A)/\partial\Phi|_\psi$ and $\partial(F_{\text{poly}}/A)/\partial\psi|_\Phi$ are all continuous] at a crossover where $\xi_3=\sigma r$, where σ is a numerical prefactor. This yields two coupled equations

$$\tfrac{9}{4}\beta\sigma+3\rho\sigma^2-\delta\sigma^{8/3}-3\eta=0,\quad \tfrac{5}{4}\beta\sigma+5\rho\sigma^2-\tfrac{10}{3}\delta\sigma^{8/3}=0. \tag{16}$$

In our discussion of the polymer free energy in the limit $r\gg\xi_3$, we stated that the system could be viewed as, essentially, a bulk solution confined between two independent parallel plates. The constants β and ρ are thus not arbitary and, in fact, their values are fixed by the bulk solution properties [the constant β is related to the osmotic pressure of a bulk polymer solution, whereas ρ can be calculated within the Cahn–de Gennes scaling functional approach[12,14] by considering depletion near a single surface (see Appendices A and B, respectively)]. If we also regard the constant σ (prefactor in the three-dimensional to two-dimensional crossover, $\xi_3=\sigma r$) as fixed, then we can consider the prefactors δ and η as being set by the matching criteria of Eq. (16). This gives the following results:

$$\delta=\tfrac{3}{8}\beta\sigma^{-5/3}+\tfrac{3}{2}\rho\sigma^{-2/3},\quad \eta=\tfrac{5}{8}\beta\sigma+\tfrac{1}{2}\rho\sigma^2. \tag{17}$$

Substituting the above expressions for δ and η into the free energy expression of Eq. (15) now gives the free energy per unit area as

$$\frac{F_{\text{poly}}a^2}{AT}=\left[\beta\left(\frac{L}{a}\right)\frac{\Phi^{9/4}}{\psi(1-\psi)^{5/4}}+2\rho\frac{\Phi^{3/2}}{(1-\psi)^{3/2}}\right],\quad \text{for } \left(\frac{L\sigma}{a}\right)^4\Phi^3\geqslant\frac{\psi^4}{(1-\psi)}$$

$$=\left[\left(\frac{3}{8}\beta\sigma^{-5/3}+\frac{3}{2}\rho\sigma^{-2/3}\right)\left(\frac{a}{L}\right)^{2/3}\frac{\psi^{2/3}\Phi}{(1-\psi)^{5/3}}+\left(\frac{5}{8}\beta\sigma+\frac{1}{2}\rho\sigma^2\right)\left(\frac{L}{a}\right)^2\frac{\Phi^3}{\psi^2(1-\psi)}\right],\quad \text{for } \left(\frac{L\sigma}{a}\right)^4\Phi^3<\frac{\psi^4}{(1-\psi)}, \tag{18}$$

where we have rewritten ξ_3 and r in terms of the volume fractions Φ and ψ.

For the consideration of phase equilibria, it is convenient to work with the free energy density rather than the free energy per unit area. Using the repeat distance of the lamellar system L/ψ, we obtain $F_{\text{poly}}/V=(F_{\text{poly}}/A)\cdot(\psi/L)$. Finally, the polymer free energy density can be written in suitably reduced units as $(F_{\text{poly}}\sigma^3L^3)/(V\beta T)=f_{\text{poly}}$, where

$$f_{\text{poly}}=\left[\frac{\Phi'^{9/4}}{(1-\psi)^{5/4}}+2\rho'\frac{\psi\Phi'^{3/2}}{(1-\psi)^{3/2}}\right]\quad \text{for } \Phi'^3\geqslant\frac{\psi^4}{(1-\psi)}$$

$$=\left[\left(\frac{3}{8}+\frac{3}{2}\rho'\right)\frac{\psi^{5/3}\Phi'}{(1-\psi)^{5/3}}+\left(\frac{5}{8}+\frac{1}{2}\rho'\right)\frac{\Phi'^3}{\psi(1-\psi)}\right] \tag{19}$$

$$\text{for } \Phi'^3<\frac{\psi^4}{(1-\psi)},$$

where we have introduced the reduced polymer volume fraction Φ' and a constant ρ' defined, respectively, by $\Phi'=(L\sigma/a)^{4/3}\Phi$ and $\rho'=(\rho\sigma)/\beta$. This completes our determination of the contribution of nonadsorbing polymer to the free energy of a lamellar phase. The ratio ρ/β is estimated in Appendix B as 0.5; this fixes ρ' as 0.5σ, so that f_{poly} contains only one unknown numerical parameter, σ itself. (For definiteness, this will be set to unity in the numerical work described below.)

C. Effect of adding nonadsorbing polymer to an unbound lamellar phase

In this section, we consider a lamellar phase governed by a strong Helfrich repulsion, which would always be unbound in the absence of polymer. Without added polymer, the free energy per unit area for such a system can be written as[15]

$$\frac{F_{\text{Helf}}}{A}=\frac{3\pi^2}{128}\frac{T^2}{K}\frac{1}{r^2}, \tag{20}$$

where K is the mean curvature rigidity of the bilayers. Rewriting r in terms of the surfactant volume fraction ψ, according to Eq. (13), and multiplying the free energy per unit area by ψ/L, gives the surfactant free energy per unit volume as

$$\frac{F_{\text{Helf}}}{V}=\frac{3\pi^2}{128}\frac{T^2}{K}\frac{\psi^3}{L^3(1-\epsilon\psi)^2}. \tag{21}$$

Here we have generalized the expression by introducing a phenomenological parameter ϵ. If ϵ is set to unity, we re-

cover the usual form for the Helfrich term; more generally, ϵ fixes an "effective" bilayer thickness ϵL which may differ from the geometrical one. Variation of ϵ thus enables us to include, at least at the phenomenological level, short-ranged repulsive or attractive forces (by setting $\epsilon > 1$ or $\epsilon < 1$, respectively). Finally, we rewrite Eq. (21) in its reduced form using the units introduced in Sec. II B

$$f_{\text{Helf}} = \frac{F_{\text{Helf}} \sigma^3 L^3}{V \beta T} = \frac{\psi^3}{k(1-\epsilon\psi)^2}, \tag{22}$$

where a reduced elastic constant k has been defined by

$$k = \frac{128}{3\pi^2} \frac{\beta K}{T\sigma^3}. \tag{23}$$

We now imagine replacing the pure solvent in the lamellar phase with our nonadsorbing polymer solution and consider the resulting phase equilibria. As discussed in Sec. I, we assume that the polymeric effect on the elastic moduli of the bilayers can be neglected and within the additive framework we merely add the polymer free energy to the Helfrich free energy

$$f = f_{\text{poly}} + f_{\text{Helf}}, \tag{24}$$

where f_{poly} and f_{Helf} are given by Eqs. (19) and (22), respectively.

To determine the phase equilibria, we must globally minimize the free energy subject to the constraint that the total amount of surfactant and polymer is fixed. Miscibility gaps are found by a common tangent construction—n phases coexist if it is possible to construct a tangent plane that touches the free energy surface at n points, but otherwise lies everywhere below it. Common tangency to the free energy surface $f(\Phi', \psi)$ is found by demanding a common value at all points of tangency for each of the following three quantities:

$$\left.\frac{\partial f}{\partial \Phi'}\right|_{\psi}, \quad \left.\frac{\partial f}{\partial \psi}\right|_{\Phi'}, \quad \text{and} \quad f - \Phi' \left.\frac{\partial f}{\partial \Phi'}\right|_{\psi} - \psi \left.\frac{\partial f}{\partial \psi}\right|_{\Phi'}. \tag{25}$$

However, if we view the minimization of f as a purely mathematical problem, then more care must be taken along the boundaries of the free energy surface, i.e., the axes $\Phi' = 0$ and $\psi = 0$. Consider the case where the coexisting phase x lies on one of these axes. It is not necessary in such a case for the plane that joins coexisting phases to be a tangent at x; this type of tangency is referred to as "virtual."[16] To demonstrate the principle of virtual tangency, let us consider the simpler case of a two component system (e.g., surfactant in water) with a free energy density $f(\psi)$ as sketched in Fig. 3. In this case, there is a coexistence between a state with $\psi = 0$ and a state with nonzero ψ. The composition of the dense phase is governed by the single coexistence equation

$$f(0) = f(\psi) - \psi \frac{df}{d\psi} \tag{26}$$

and the equality of chemical potentials $df/d\psi$ is not necessary. Geometrically, the criterion is equivalent to finding a line which goes through the origin $f(0)$ and is at some point tangent to the free energy, but otherwise lies below it; the point of tangency defines the composition of the dense phase.

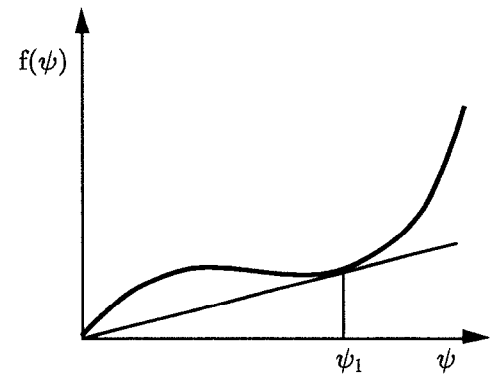

FIG. 3. The virtual tangent construction for the free energy $f(\psi)$; the point of contact defines the composition of the dense phase ψ_1.

Physically, the need to consider virtual tangency with states where $\Phi' = 0$ or $\psi = 0$ (or both) is a result of our free energy being inaccurate in the limit of small Φ' and ψ. In our model, we assume that as $\psi \to 0$, the surfactant structure remains lamellar; however, in this dilute region, the surfactant will probably exist in the form of micelles or isolated molecules in solution.[16] Also, our assumption that the polymer is under semidilute conditions in the solvent allowed us to neglect the translational entropy of the chains, whereas for dilute conditions, the translational entropy should really be included. If the dilute phases were described more accurately, virtual tangencies would become real tangencies where the composition of the dilute phase would be exponentially small.[16] At the level of our model, however, the description of the dilute Φ' and ψ limit is adequate, as long as we allow for possible virtual tangencies to points on the boundary of the phase diagram when applying the coexistence criteria of Eq. (25).

As mentioned above, the parameter ρ' in f_{poly} is fixed by the procedure of Appendix B as $\rho' = 0.5\sigma$, whereas the prefactor σ cannot be easily determined, and for definiteness, we set it to unity (so that the crossover from three-dimensional to two-dimensional polymer behavior occurs when $\xi_3 = r$). The reduced free energy density f of Eq. (24) is just a function of Φ', ψ, ϵ, and k, enabling us to determine the phase diagram in the composition plane (Φ', ψ) for a given k and ϵ. The calculation of the phase diagram is fairly straightforward.

Three calculated phase diagrams, for various values of k with $\epsilon = 1$, are shown in Figs. 4(a)–4(c). For $k = 50$ [Fig. 4(a)], the system is immiscible; the polymer does not enter the lamellar phase, but is ejected as a semidilute solution. For some critical k ($k \simeq 23.5$ for our choice of parameters), a *line* of three-phase coexistence arises (pure lamellar phase + mixed polymer–lamellar + pure polymer solution) [Fig. 4(b)]. This three phase line is something of an artifact; we discuss it shortly. As k is decreased further, the phase diagram splits into immiscible and miscible regions as shown Fig. 4(c).

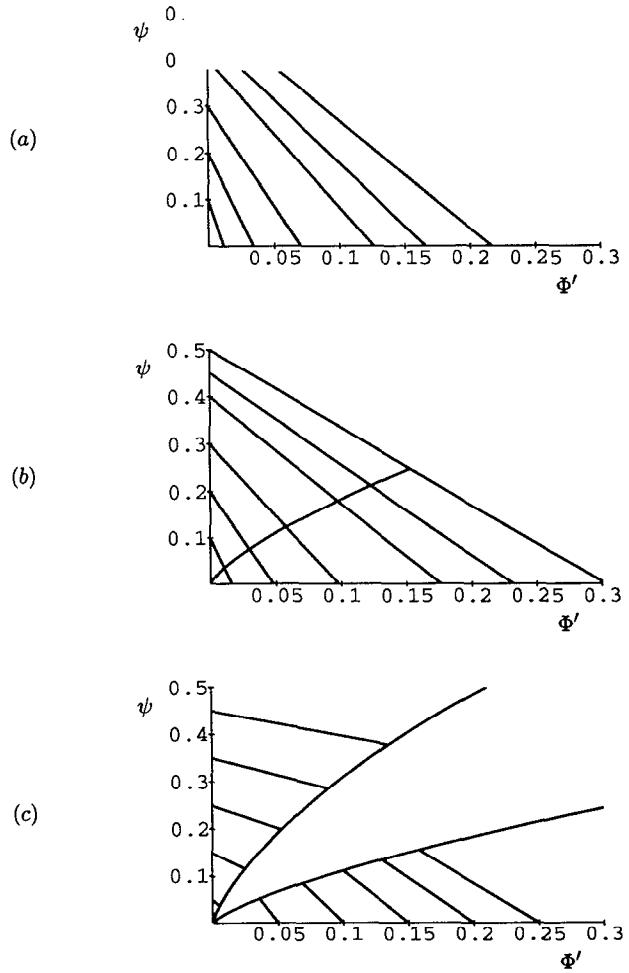

FIG. 4. Calculated phase diagrams for the Helfrich-stabilized, nonadsorbing polymer–lamellar system. (Horizontal scale) the reduced polymer volume fraction Φ'. (Vertical scale) the surfactant volume fraction ψ. Reduced mean curvature rigidity (a) $k=50$ and $\epsilon=1$; (b) $k=23.5$ and $\epsilon=1$; and (c) $k=3$ and $\epsilon=1$.

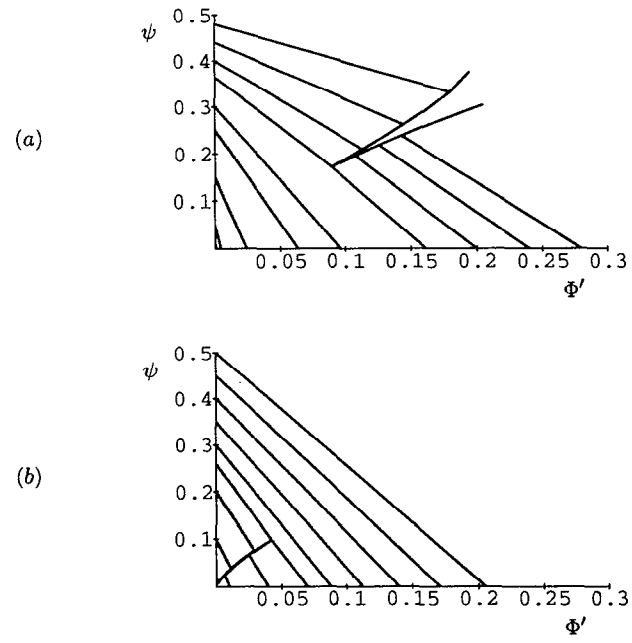

FIG. 5. Calculated phase diagrams for the Helfrich-stabilized, nonadsorbing polymer–lamellar system with $\epsilon\neq1$. (Horizontal scales) the reduced polymer volume fraction Φ'. (Vertical scales) the surfactant volume fraction ψ. Reduced mean curvature rigidity (a) $k=50$ and $\epsilon=1.5$ and (b) $k=16$ and $\epsilon=0.5$.

Using the chosen value of $\sigma=1$ and setting the polymer constant $\beta=1.97$ (Appendix A), we can translate our k parameter into the physical mean curvature rigidity K; for $k=50$, we find that $K\simeq6T$. With this rather high rigidity, the Helfrich repulsion is not sufficient to prevent the polymer from leaving the interlamellar regions with some of the solvent, hence reducing the depletion energy at the expense of significant layer compression. The system then exists as a pure surfactant lamellar phase coexisting with an excess semidilute polymer solution. In contrast, for $k=3$, we have $K\simeq0.4T$. In this case, the bilayers are very flexible and the Helfrich repulsion is much larger. In the central region of the phase diagram [see Fig. 4(c)], the system is a single polymer-containing lamellar phase, the Helfrich repulsion being sufficiently large to prevent the polymer from leaving the interlamellar regions. However, if we increase the volume fraction of polymer too much, the increased polymer depletion energy does drive a separation between polymer-containing lamellar phase and a semidilute polymer solution. A similar situation applies for large surfactant volume fractions, the phase separation (now to a polymer-free lamellar phase) again driven by the increasing entropic penalty associated with confining the polymer in very narrow layers.

Turning to the intermediate diagram [Fig. 4(b)], we found that a line of three-phase coexistence arose. Although the transition from Fig. 4(a)–4(c) requires a diagram of intermediate topology, for this to take the form shown in Fig. 4(b) is most odd. We believe the result to be an artifact of our model free energy; it turns out that for the (most natural) choice of $\epsilon=1$, the free energy f of Eq. (24) can be written as a product

$$f=\frac{\psi^3}{(1-\psi)^2}\mathcal{F}(k,z), \tag{27}$$

where $z=\Phi'^3(1-\psi)/\psi^4$. The phase boundaries in Fig. 4(c) are each loci of $z=$constant, and these collapse onto each other along their entire length for a particular value of z. We emphasize that this reduction in the number of degrees of freedom is rather accidental and can be overcome by setting $\epsilon\neq1$.

To see what happens when $\epsilon\neq1$, we have performed calculations of the phase diagram using the same approach as described above. We now find that the evolution of the phase diagram as a function of k depends delicately upon whether $\epsilon>1$ or $\epsilon<1$. The phase diagram for $k=50$ and $\epsilon=1.5$ is shown in Fig. 5(a); this value of ϵ should correspond to having short-ranged repulsions (e.g., hydration forces). As can be seen, the phase diagram now shows a one-phase region for large Φ' and ψ which ends in a three-phase point. As k is decreased (keeping $\epsilon=1.5$), the three-

phase point moves towards the origin and the one-phase region "opens out" approaching that of Fig. 4(c). The stabilization of a single phase at high volume fractions of surfactant is what one would expect if additional short-range repulsions are present.

On the other hand, if $\epsilon=0.5$ (short-ranged attractions), we find that for large k, the one-phase region is located near the origin. As k is decreased, the three-phase point (marking the end of the one-phase region) moves towards larger Φ' and ψ, and the one-phase region again spreads out; a phase diagram calculated for $k=16$ and $\epsilon=0.5$ is shown in Fig. 5(b). Thus, for short-range attractions, the stability of a single phase at large volume fractions is reduced. The unexpected dependence of our results on ϵ show a remarkable sensitivity of the phase equilibria to quite detailed features of the membrane interactions.

D. The effect of adding nonadsorbing polymer to a bound lamellar system

We now consider the effects of adding nonadsorbing polymer to a lamellar phase in which the attractive van der Waals interaction between bilayers produces a bound state; adding more solvent fails to swell the phase. Within the additive model, we assume that complete collapse of the lamellar structure, due to these attractive interactions, is prevented by short-ranged repulsive forces, e.g., hydration; in the absence of polymer, the equilibrium interlamellar spacing is determined by a balance between the two. The free energy per unit area for a lamellar system with van der Waals and hydration interactions can be written as[17]

$$\frac{F_{\mathrm{vdW}}}{A}=-\frac{W}{12\pi}\left[\frac{1}{r^2}-\frac{2}{(r+L)^2}+\frac{1}{(r+2L)^2}\right]+F_0e^{-r/\lambda_H}, \tag{28}$$

where W is the Hamaker constant and is typically of order T, F_0 is a constant, and λ_H is a microscopic length (typically 2–3 Å). Rewriting r in terms of the surfactant volume fraction ψ, according to Eq. (13), and multiplying the free energy per unit area by ψ/L, gives the free energy density for the bound phase in reduced units as $(F_{\mathrm{vdW}}\sigma^3L^3)/(V\beta T)=f_{\mathrm{vdW}}$, where

$$f_{\mathrm{vdW}}=-w\psi^3\left[\frac{1}{(1-\psi)^2}-2+\frac{1}{(1+\psi)^2}\right]+f_0\psi\exp\left[-\frac{(1-\psi)}{\psi}\frac{L}{\lambda_H}\right] \tag{29}$$

with $w=(W\sigma^3)/(12\pi\beta T)$ and $f_0=(F_0\sigma^3L^2)/(\beta T)$.

As in the unbound case studied in Sec. II C, we now replace the pure solvent in the lamellar phase with a nonadsorbing polymer solution and consider the resulting phase equilibria. The addition of Eq. (29) to the polymer free energy of Eq. (19) gives the total reduced free energy density f. The calculation of the phase diagram follows the same strategy as before—for a given w, f_0, and λ_H/L, we apply the common tangent criteria of Eq. (25) to the free energy f (allowing for virtual tangency with phases where $\Phi'=0$, $\psi=0$, or both). The resulting coexistence equations are again solved numerically to obtain the phase diagram.

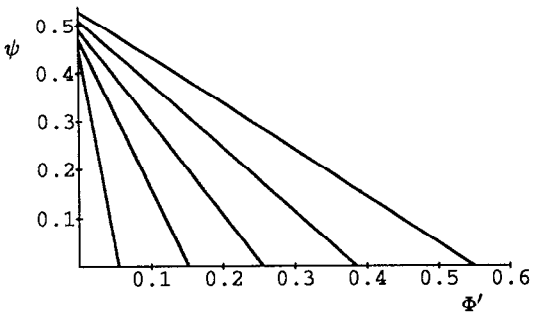

FIG. 6. Calculated phase diagram for the van der Waals+hydration-stabilized, nonadsorbing polymer–lamellar system. (Horizontal scale) the reduced polymer volume fraction Φ'. (Vertical scale) the surfactant volume fraction ψ. Parameter values $w=0.013$; $f_0=250$; and $\lambda_H/L=0.1$.

A calculated phase diagram for $w=0.013$, $f_0=250$, and $\lambda_H/L=0.1$ is shown in Fig. 6. We have chosen values for the parameters f_0 and λ_H/L which are comparable to those used by Lipowsky and Leibler,[2] and the reduced Hamaker constant $w=0.013$ corresponds to a physical Hamaker constant of $W\simeq 1T$. As can be seen in Fig. 6, the system exists as a bound lamellar phase coexisiting with a semidilute polymer solution. If we start with a pure solvent, then the lamellar phase is bound with a maximum volume fraction (with the above choice of parameter values) of $\psi\simeq 0.45$. Upon addition of the polymer, we find that the chains remain in the excess solvent and do not infiltrate the lamellar structure. The polymer applies an osmotic pressure to the lamellar phase; the interlamellar spacing is then reduced, giving an increase in the volume fraction ψ. Adding more polymer simply increases the applied osmotic pressure and increases the value of ψ in the lamellar phase. The effect of varying W is to give phase diagrams which are qualitatively similar to that of Fig. 6; the value of ψ in the lamellar phase depends on W, but the system still exists as a bound lamellar phase coexisting with a semidilute polymer solution.

These results are relevant to the measurement of membrane interactions using osmotic pressure techniques, as pioneered by Parsegian *et al.*[18] In this experimental approach, the interactions between bilayers in a *bound* lamellar phase are measured by adding polymer to the excess solvent so as to alter the osmotic pressure. Usually there is no semipermeable membrane between the solvent and the lamellar phase; one simply assumes the polymers do not penetrate it. As one might expect, our calculation shows this to be valid for nonadsorbing polymers. However, in the adsorbing case, the situation is different and we return to this in Sec. III C.

III. ADSORBING POLYMER

So far we have studied the effect of adding nonadsorbing polymer to unbound and bound lamellar phases. In this section, we consider the effects of instead adding polymer which has an affinity to the bilayer surface. In this case, it is not possible to formulate a simple estimate for the polymer free energy using blob concepts, as was done for non-

adsorbing polymer. However, if we continue to regard each bilayer as a flat impenetrable surface (for the purposes of calculating the polymer contribution), then we can use the Cahn–de Gennes scaling functional approach[12,14] to find the free energy, in terms of a few fundamental parameters. We continue to restrict attention to good solvent conditions for the polymeric species. As discussed in Sec. I, we ignore any effect of polymer on renormalization of the elastic moduli, and focus on the "direct" polymer contribution to the free energy. This should be adequate providing we consider reasonably stiff bilayers ($K \gg T$) and avoid conditions of very strong adsorption.

A. Polymer free energy

1. Choice of adsorption parameters

We first consider adsorption onto a *single* planar surface from a very dilute bulk polymer solution. The corresponding free energy per unit area is given by the de Gennes functional which is of mean-field type, but incorporates the correct scaling exponents for a good solvent[12]

$$\frac{F_{\text{poly}}}{A}=\gamma_0-\gamma_1\phi_{s0}+\frac{\beta T}{a^3}\int_0^\infty\left[\phi^{-5/4}\left(m_0\frac{d\phi}{dz}\right)^2+\phi^{9/4}\right]dz, \tag{30}$$

where γ_0 is the surface energy of the pure solvent, γ_1 is the monomeric sticking energy, a is a monomeric length scale, ϕ is the local volume fraction of polymer in the solvent (ϕ_{s0} is the value of ϕ at the surface), and m_0 and β are universal constants ($m_0^2=\alpha a^2/\beta$, where α is as defined in Appendix A). Minimization of Eq. (30) gives the profile equation and a boundary condition at the surface

$$\phi^{-5/4}\left(m_0\frac{d\phi}{dz}\right)^2-\phi^{9/4}=0, \tag{31}$$

$$\left(\frac{1}{\phi^{5/4}}\frac{d\phi}{dz}\right)_{z=0}=-\frac{\gamma_1 a^3}{2\beta T m_0^2}. \tag{32}$$

From the boundary condition at the surface arises a length scale, the "extrapolation length" D,[12,14] which is defined by $1/D=|1/\phi\cdot(d\phi/dz)|_{z=0}$, giving

$$\frac{1}{D}=\frac{\gamma_1 a^3}{2\beta T m_0^2}\phi_{s0}^{1/4}, \quad \text{where } \phi_{s0}=\left(\frac{m_0}{D}\right)^{4/3}. \tag{33}$$

As can be seen from Eq. (33), the surface volume fraction ϕ_{s0} is a unique function of D. The length scale D and the surface volume fraction ϕ_{s0}, which pertain to the properties of a single surface in contact with bulk solution, are convenient parameters with which to characterize the adsorption, allowing reduced variables to be introduced as shown below.

2. Formulation of the free energy

We now consider two bilayers (which we approximate as flat) a distance r apart. The polymer free energy per unit area is [cf. Eq. (30)]

$$\frac{F_{\text{poly}}}{A}=2\gamma_0-2\gamma_1\phi_s+\frac{\beta T}{a^3}\int_0^r\left[\phi^{-5/4}\left(m_0\frac{d\phi}{dz}\right)^2+\phi^{9/4}\right]dz. \tag{34}$$

The average monomer volume fraction $\bar{\phi}$ in the solvent obeys $\bar{\phi}=1/r\cdot\int_0^r\phi\,dz$; we treat this as a constraint, and find the profile by minimizing $\bar{F}_{\text{poly}}/A=F_{\text{poly}}/A-\lambda\bar{\phi}$, where λ is a Lagrange multiplier. We write

$$\frac{\bar{F}_{\text{poly}}}{A}=2\gamma_0-2\gamma_1\phi_s+\frac{\beta T}{a^3}\int_0^r\left[\phi^{-5/4}\left(m_0\frac{d\phi}{dz}\right)^2+\phi^{9/4}-\lambda'\phi\right]dz, \tag{35}$$

where $\lambda'=\lambda a^3/\beta T r$. It is useful to introduce a reduced variable $g(z)$, defined by $g=\phi^{3/8}$, rewriting Eq. (35) as

$$\frac{\bar{F}_{\text{poly}}}{A}=2\gamma_0-2\gamma_1 g_s^{8/3}+\frac{\beta T}{a^3}\int_0^r\left[\left(m\frac{dg}{dz}\right)^2+g^6-\lambda' g^{8/3}\right]dz, \tag{36}$$

where $m=8m_0/3$.

Minimizing $\bar{F}_{\text{poly}}/A$ with respect to changes in the profile gives the profile equations as

$$\left(m\frac{dg}{dz}\right)^2=(g^6-g_m{}^6)-\lambda'(g^{8/3}-g_m{}^{8/3}), \tag{37}$$

$$\frac{8}{3}\left|\left(\frac{g_{s0}}{g}\right)^{2/3}\left(\frac{1}{g}\frac{dg}{dz}\right)\right|_{z=0,r}=\frac{1}{D}, \tag{38}$$

where g_m is the value of g at the midpoint between the two bilayers (where by symmetry dg/dz vanishes) and $g_{s0}=\phi_{s0}^{3/8}$ with ϕ_{s0} defined in Eq. (33). It is now convenient to normalize g by the midpoint value g_m, introducing $y=(g/g_m)^{2/3}$, and to measure all lengths in units of the extrapolation length D, e.g., $z=D\tilde{z}$. Writing $\lambda'=\mu g_m^{10/3}$ enables Eqs. (37) and (38) to be expressed in reduced units as

$$\left(\frac{dy}{d\tilde{z}}\right)^2=\frac{1}{16yy_{s0}^6}[(y^9-1)-\mu(y^4-1)], \tag{39}$$

$$1=4\left|\left(\frac{y_{s0}}{y}\right)\left(\frac{1}{y}\frac{dy}{d\tilde{z}}\right)\right|_{\tilde{z}=0,\tilde{r}}, \tag{40}$$

where $y_{s0}=(g_{s0}/g_m)^{2/3}=(\phi_{s0}/\phi_m)^{1/4}$. It should be noted that in this choice of units, y_{s0} is not a constant. We can express y_{s0} as a function of the normalized surface concentration y_s and the chemical potential μ by substituting Eq. (39) into Eq. (40), giving

$$y_{s0}=y_s\Delta^{1/2}(y_s), \quad \text{where } \Delta^2(x)\equiv 1-\mu x^{-5}+(\mu-1)x^{-9}. \tag{41}$$

To determine the polymer free energy for a given average polymer volume fraction $\bar{\phi}$ and interlamellar spacing r, we need to determine the parameters y_s and μ. Integrating the profile equation (39) gives one relation between y_s and μ,

$$\tilde{r}=8y_s^3\Delta^{3/2}(y_s)\int_1^{y_s}y^{-4}\Delta^{-1}(y)dy. \tag{42}$$

A second relation can be determined from the imposed constraint, namely, the average polymer volume fraction in the solvent which, in the reduced units, is given by

$$\bar{\phi}=\frac{8}{\tilde{r}}\phi_{s0}y_s^{-1}\Delta^{-1/2}(y_s)\int_1^{y_s}\Delta^{-1}(y)dy. \tag{43}$$

Equations (42) and (43) are enough to completely determine y_s and μ, and hence the free energy, for a particular $\bar{\phi}$ and $\tilde{r}$.

This completes the formal procedure for finding the polymeric contribution to the free energy. However, just as in Sec. II C, in order to calculate phase diagrams, we must re-express these results in terms of our fundamental composition variables—the volume fraction of polymer Φ and volume fraction of surfactant ψ. The relations among $\bar{\phi}$, r, Φ, and ψ are given by (see Sec. II C)

$$\Phi=\bar{\phi}(1-\psi) \quad \text{and} \quad \frac{r}{L}=\frac{(1-\psi)}{\psi}. \tag{44}$$

Using these expressions {and writing ϕ_{s0} in terms of the extrapolation length D [Eq. (33)]}, we can rewrite Eqs. (42) and (43), giving the coupled equations for y_s and μ in terms of Φ and ψ as

$$\frac{L}{D}\frac{(1-\psi)}{\psi}=8y_s^3\Delta^{3/2}(y_s)\int_1^{y_s}y^{-4}\Delta^{-1}(y)dy,$$

$$\frac{L}{D}\frac{\Phi'}{\psi}=8y_s^{-1}\Delta^{-1/2}(y_s)\int_1^{y_s}\Delta^{-1}(y)dy, \tag{45}$$

where we have introduced a reduced polymer volume fraction Φ', defined by

$$\Phi'=\left(\frac{m_0}{D}\right)^{-4/3}\Phi. \tag{46}$$

Finally, the polymer contribution to the free energy density can be determined from $\bar{F}_{\text{poly}}/A$ by inverting the Legendre transform, giving (in suitably reduced units)

$$f_{\text{poly}}=\frac{F_{\text{poly}}L^3}{V\beta(m_0/a)^3T}$$
$$=\left(\frac{L}{D}\right)^2\psi\left\{-4\Delta^{-2}(y_s)\right.$$
$$\left.+\frac{8}{y_s^6\Delta^3(y_s)}\int_1^{y_s}y^5[\Delta(y)+\Delta^{-1}(y)]dy\right\}, \tag{47}$$

where we have dropped the $2\gamma_0$ term since its contribution to the free energy density is linear in ψ, and thus it will have no effect on the phase behavior of the system. Note that the definition of the reduced unit of free energy differs slightly (by an order unity constant) from that used in Sec. II above. Since we never have to consider direct equilibria between phases of adsorbing and nonadsorbing polymer, this does not matter.

B. The effect of adding adsorbing polymer to an unbound lamellar system

In this section, we consider the effects of adding adsorbing polymer to a Helfrich-stabilized lamellar phase. As in the nonadsorbing case of Sec. II C, we add the polymer free energy density of Eq. (47) to the surfactant free energy contribution [see Eq. (21) of Sec. II C] to give the total free energy density f. In the present units, the Helfrich contribution has the form

$$f_{\text{Helf}}=\frac{F_{\text{Helf}}L^3}{V\beta(m_0/a)^3T}=\frac{\psi^3}{k(1-\epsilon\psi)^2}, \tag{48}$$

where the reduced rigidity k is now defined by

$$k=\frac{128}{3\pi^2}\frac{\beta}{T}\left(\frac{m_0}{a}\right)^3K. \tag{49}$$

(Note: this differs from that of Sec. II by an order unity factor.)

To calculate the phase diagram, we proceed as before. Application of the coexistence criteria of Eq. (25) to the reduced free energy density f gives the equations for phase equilibria. The solution of the coexistence equations is again achieved numerically, allowing for virtual tangencies (see Sec. II C). However, the calculation is somewhat more involved than that for the nonadsorbing case considered previously since f_{poly} is a much more complicated expression. Phase diagrams in the composition plane (Φ,ψ) were found for various values of the ratio D/a (adsorption strength) and the reduced rigidity k (strength of the Helfrich repulsion). Throughout we have used a bilayer thickness to monomer length-scale ratio of $L/a=5$ and have set $\epsilon=1$ [variation of ϵ from its unity value does not qualitatively affect the phase diagram in contrast to the nonadsorbing system, where $\epsilon\neq1$ was necessary to remove a spurious factorability of the free energy density (see Sec. II C)].

Three calculated phase diagrams are shown in Fig. 7. In Fig. 7(a), we have used the following parameter values: $D/a=5$ and $k=1$. Using the theoretical estimates of the universal polymer constant $\beta=1.97$ and $m_0/a=0.23$ (Appendix A), we calculate that the unscaled rigidity for this k value is $K\simeq10T$. The phase diagram consists of a two-phase and a one-phase region, the two-phase region terminating at a critical point. The two-phase region is composed of three distinct parts. At the left-hand edge of the figure, coexistence is between a polymer-containing lamellar phase and pure solvent. The central region (intermediate Φ) shows coexistence between a polymer-containing lamellar phase and a semidilute polymer solution. Finally, at high Φ, there is coexistence between two polymer-containing lamellar phases. The first two regions involve virtual tangency to the edges of the phase diagram. Using an improved estimate for the free energy density at low volume fractions would ensure that coexisting phases contained finite (if only exponentially small) concentrations of both polymer and surfactant.

The form of the phase diagram shown in Fig. 7(a) can be understood by considering the force between two sur-

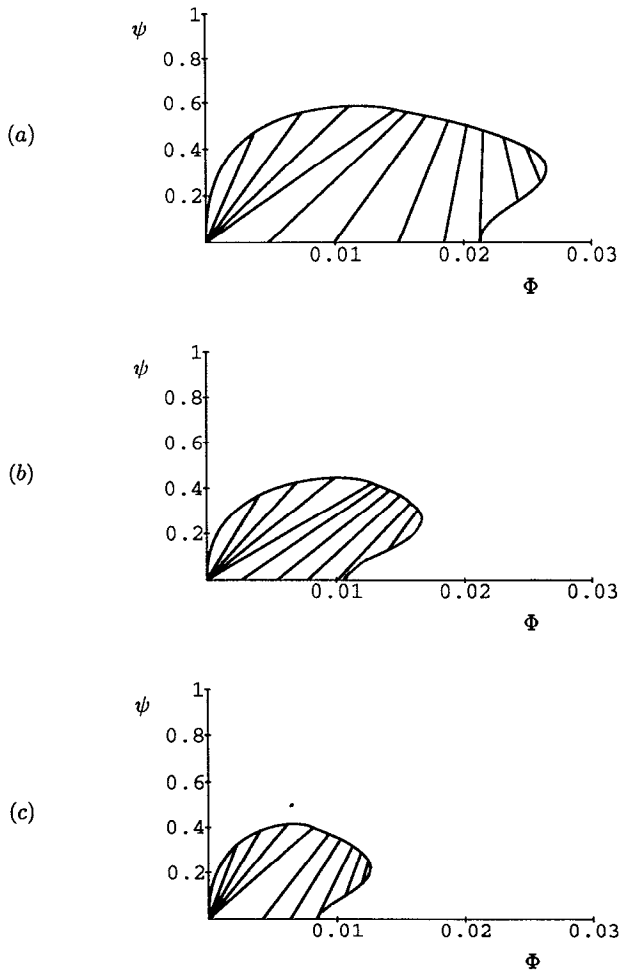

FIG. 7. Calculated phase diagrams for the Helfrich-stabilized, adsorbing polymer–lamellar system. Parameter values for (a); (b); and (c) $L/a=5$ and $\epsilon=1$. (Horizontal scale) physical polymer volume fraction Φ. (Vertical scale) the surfactant volume fraction ψ. (a) Reduced mean curvature rigidity $k=1$ and adsorption strength $D/a=5$; (b) reduced mean curvature rigidity $k=0.5$ and adsorption strength $D/a=5$; and (c) reduced mean curvature rigidity $k=1$ and adsorption strength $D/a=10$.

faces bearing adsorbed polymer. This depends delicately on the amount adsorbed (surface coverage) and the nature of the equilibrium governing the polymer chains. In calculating the polymer free energy in a homogeneous polymer-containing lamellar phase, we used the fact that the polymer chains are confined to remain in the interlamellar region. In the language of homopolymer adsorption onto solid surfaces, this would correspond to the well-studied case of "restricted equilibrium."[14] The role of surface coverage on the force between two surfaces bearing adsorbed polymer layers, within the restricted equilibrium model, was investigated by Rossi and Pincus.[19] They found that for surface coverages equal to, or above, some optimum value (referred to as saturated), the force is *always* repulsive;[19] excluded-volume interactions dominate. In contrast, if the surface coverage is below its optimum, then the force has an *attractive* tail at large intersurface separations[19] caused by polymer chains bridging the gap between the surfaces.

Returning now to the polymer–lamellar system, we can envisage that if the added volume fraction of polymer is sufficiently low (below the optimum coverage), then the presence of attractive polymer-mediated forces may be sufficient to overcome the repulsive Helfrich interaction and produce a bound lamellar phase. This is consistent with Fig. 7(a). As more polymer is added to the system, the repulsive excluded-volume interaction becomes more important, dominating the attractive bridging forces. At sufficiently large volume fractions of semidilute polymer, the excluded volume interaction dominates the attraction of monomers to the surfaces and the adsorption is relatively weak. The volume fraction profile in the intersurface regions is then approximately flat. In this case, we would expect the "bare" surfactant-mediated interaction to determine the nature of the phase equilibria, i.e., the system would be unbound due to the repulsive Helfrich interaction. This is also consistent with the calculated phase diagram of Fig. 7(a).

The effects of varying the strength of adsorption D/a and the rigidity k are qualitatively as predicted from the above physical picture. The phase diagram shown in Fig. 7(b) demonstrates the effects of reducing the rigidity from $k=1$ to $k=0.5$ (still keeping $D/a=5$). The increased Helfrich repulsion shifts the boundary of the two-phase region to smaller polymer and surfactant volume fractions. Likewise, if we reduce the strength of the polymer adsorption from its value in Fig. 7(a) (still keeping $k=1$), we obtain the phase diagram shown in Fig. 7(c). The strength of the attractive polymer-bridging forces between adjacent lamellae is now reduced and the boundary of the two-phase region is again shifted to smaller volume fractions.

C. The effect of adding adsorbing polymer to a bound lamellar system

As discussed in Sec. II D, the free energy density for a lamellar system governed by van der Waals and hydration interactions can be written in reduced units as

$$f_{\mathrm{vdW}}=\frac{F_{\mathrm{vdW}}L^3}{V\beta(m_0/a)^3T}$$
$$=-w\psi^3\left[\frac{1}{(1-\psi)^2}-2+\frac{1}{(1+\psi)^2}\right]$$
$$+f_0\psi\exp\left[-\frac{(1-\psi)}{\psi}\frac{L}{\lambda_H}\right], \qquad (50)$$

where $w=W/[12\pi\beta(m_0/a)^3T]$ and $f_0=(F_0L^2)/[\beta(m_0/a)^3T]$. (Note that these definitions differ from those of Sec. II D by an order unity factor.) In the presence of adsorbing polymer, the addition of Eq. (50) to the polymer free energy of Eq. (47) now gives the total reduced free energy density f.

The calculation of the phase diagram follows as before: for a given w, f_0, λ_H/L, D/a, and L/a, we apply the common tangent criteria of Eq. (25) to the free energy f (allowing for virtual tangency to phases where $\Phi'=0$, $\psi=0$, or both). A numerically calculated phase diagram for $w=1.18$, $f_0=22\,000$, $\lambda_H/L=0.1$, and $D/a=5$ is

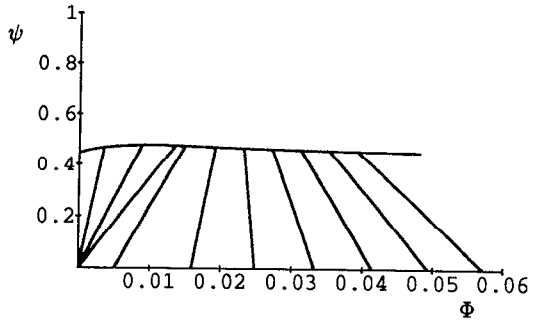

FIG. 8. Calculated phase diagram for the van der Waals+hydration-stabilized, adsorbing polymer–lamellar system. (Horizontal scale) the physical polymer volume fraction Φ. (Vertical scale) the surfactant volume fraction ψ. Parameter values $L/a=5$, $D/a=5$, $w=1.18$, $f_0=22\,000$, and $\lambda_H/L=0.1$.

shown in Fig. 8 (as in Sec. III B, we use a bilayer thickness to monomer size ratio of $L/a=5$). Again, we have chosen values for the parameters f_0 and λ_H/L which are comparable to those used by Lipowsky and Leibler,[2] and the reduced Hamaker constant $w=1.18$ corresponds to a physical Hamaker constant of $W\simeq 1T$. The phase diagram shows both a one-phase and a two-phase region. The latter consists of two distinct parts—a polymer-containing lamellar phase coexisting with pure solvent, and a polymer-containing lamellar phase coexisting with a polymer solution. These both involve virtual tangencies and the same comments apply here as in the discussion of Fig. 7 given above.

The form of the phase diagram can again be explained by considering the polymer-mediated interaction between adjacent lamellae. Starting with pure solvent (no polymer) and with the above parameter values, the system is bound; the surfactant volume fraction in the bound phase is $\psi\simeq 0.45$. The addition of a small quantity of polymer (where the polymer coverage is below its optimum) will produce attractive bridging forces between adjacent lamellae, reducing the equilibrium interlamellar spacing, and thus the surfactant volume fraction in the bound phase should be increased. In the opposite limit of large polymer volume fractions, the adsorbing nature of the surface will become unimportant and the polymer density will approach a flat profile. In this case, the bare surfactant-mediated interaction will determine the phase equilibria, and thus the value of ψ on the two-phase boundary should decrease and tend towards the pure solvent value of $\psi\simeq 0.45$. The above interpretation agrees qualitatively with the calculated phase diagram, though the shift in the surfactant volume fraction in the bound phase is never very large. Varying the strength of adsorption D/a or the Hamaker constant W affects the composition of the coexisting phases, but the phase diagram remains qualitatively as described above.

These results show that adsorbing polymer can be significantly partitioned from solution into a bound lamellar phase. In any attempt to measure the osmotic pressure of such phases by putting them in direct contact with a polymer solution,[18] it is obviously important to use nonadsorbing polymer.

IV. SUMMARY AND DISCUSSION

We have above determined, for various cases, the effects of adding homopolymer to a lamellar phase. In previous work,[6,7] we demonstrated that the shift in the elastic moduli due to added polymer is normally small compared to bare surfactant elastic moduli, and hence in our calculations we have neglected this effect. The polymer was thus regarded as producing an interlamellar interaction which was a function of the layer spacing, the amount of added polymer, and depended on the nature of the polymer–bilayer interaction. This interaction was simply added to those already present in the lamellar phase. Although this additive model has serious shortcomings—especially near the critical unbinding transition, as discussed in the Introduction—we consider it reasonable for a first approach to this important problem. (The polymeric effect on the critical unbinding transition could, in principle, be investigated by adopting the approach of Milner and Roux.[4] However, the calculations would be quite complicated.) The effects of adding nonadsorbing and adsorbing polymer to unbound (Helfrich) and bound (van der Waals/hydration) lamellar mesophases were calculated on the basis of the additive model, and corresponding phase diagrams presented. To summarize briefly:

(1) Unbound lamellar phase+nonadsorbing polymer. For stiff bilayers ($K\simeq 5T$), the polymer is expelled as a semidilute solution. This causes the layer spacing in the lamellar phase to decrease. For very flexible bilayers ($K\simeq 0.5T$), there is a central one-phase region where the Helfrich repulsion is sufficiently large to prevent the polymer from leaving the interlamellar regions. Phase separation to a pure lamellar phase or a polymer solution arises at high or low polymer/surfactant ratios, respectively. The evolution of the phase diagram as a function of the rigidity K was found to depend critically on the nature of short-ranged interlamellar interactions.

(2) Unbound lamellar phase+adsorbing polymer. Added polymer is always present in the lamellar phase. At small polymer fractions, the system forms a bound polymer-containing lamellar phase coexisting with pure solvent. The binding presumably arises from polymeric bridging forces. At higher polymer fractions, coexistence involves not a pure solvent, but a semidilute polymer solution. At still larger amounts of added polymer, two polymer-containing lamellar phases coexist, and the two-phase region then terminates at a critical point. Beyond this region, the polymer profile between bilayers is relatively flat and does not contribute strongly to the free energy—the system is one phase due to the repulsive Helfrich interaction. The effects of reducing the strength of adsorption or reducing the rigidity K (increasing the Helfrich interaction) is to reduce the size of the two-phase region.

(3) Bound lamellar phase+nonadsorbing polymer. The polymer never enters the lamellar phase; it coexists as a semidilute polymer solution. The interlamellar spacing is

reduced because of the osmotic pressure exerted by the external polymer solution. This effect has recently been reported by van de Pas *et al.*[20]

(4) Bound lamellar phase+adsorbing polymer. Added polymer is always present in the lamellar phase. For small amounts of added polymer, the lamellar phase coexists with pure solvent; the interlamellar spacing is decreased slightly from its pure solvent value by the presence of attractive polymer-bridging forces. As more polymer is added, coexistence is with a semidilute polymer solution. For large amounts of added polymer, the density profile between bilayers becomes flat and the polymer plays a negligible role.

In all our calculations, we have assumed any polymer present is semidilute and used the virtual tangency method to predict coexistence with phases having zero volume fraction of one or more components. Thus statements made above about (for instance) coexistence of a lamellar phase with a "pure solvent" represent physically coexistence with a "very dilute solution of polymer and surfactant" whose properties we have not tried to determine.

Throughout this paper, we have assumed that upon the addition of polymer to a lamellar system, the surfactant bilayers still prefer to form a lamellar structure. At the level of our description for the polymer–bilayer interactions, this assumption is justified; we assume that the monomers interact weakly with the bilayer without penetrating the surface. This assumption, though probably valid for homopolymers, may not be true for polymers of a more complex architecture; e.g., a copolymer with a sparse fraction of strongly adsorbing groups. As discussed above, we neglected the polymeric renormalization of the Helfrich interaction which, under most conditions of interest, should be small. However, the polymeric effect on K and on the Gaussian rigidity $\bar{K}$ could play an important role in a lamellar surfactant system for which K or $\bar{K}$ is close to a critical value at which the preferred topology is altered. Examples might include systems very close to a transition to a cubic, hexagonal, or isotropic ($L3$) phase. We leave this issue for future study.

ACKNOWLEDGMENTS

We thank C. M. Marques, A. Johner, and M. S. Turner for helpful discussions; J. T. B. thanks SERC and Unilever PLC for a CASE award.

APPENDIX A: UNIVERSAL POLYMER CONSTANTS α AND β

The de Gennes free energy functional which allows for spatial inhomogeneity in semidilute polymer solutions is formulated to obtain the correct scaling for good solvent conditions. The local free energy density F has the form [12]

$$F=\frac{T}{a^3}\left[\frac{\alpha a^2}{\phi^{4/5}(\phi+\phi_b)^{9/20}}\left(\frac{d\phi}{dz}\right)^2+\beta\phi^{9/4}\right], \tag{A1}$$

where ϕ is the local volume fraction, ϕ_b is a bulk volume fraction, a is a monomeric length scale, and α and β are universal constants. In this appendix, we determine numerical values for the constants α and β.

From Eq. (A1), it is not immediately obvious that α and β are universal, indeed the expression for F contains a and ϕ which are not independent of chemical microstructure. To make the universality of these constants apparent, we rewrite Eq. (A1) using the polymer number density C and the screening length ξ,

$$F=\frac{T}{\xi^3}\left[\alpha\left(\frac{C}{C+C_b}\right)^{9/20}\left(\frac{\nabla C}{C}\xi\right)^2+\beta\right]. \tag{A2}$$

We define ξ as (Chap. 13, Sec. 2.1 of Ref. 21)

$$\xi=X\left(\frac{C}{C^*}\right)^{-3/4}, \tag{A3}$$

where X is the mean size of the molecule (the mean square end-to-end distance $R^2=dX^2$, where $d=3$) and C^* is the overlap concentration defined by $C^*=X^{-3}$.

The constant β can be related to the osmotic pressure of a bulk polymer solution, which is written as (Chap. 13, Sec. 2.5.1 of Ref. 21)

$$\frac{\Pi}{T}=\frac{F_\infty}{\xi^3}, \tag{A4}$$

where F_∞ is a universal constant and is simply related to β by

$$\beta=\tfrac{4}{5}F_\infty. \tag{A5}$$

To determine α, we must first consider the ratio α/β. This can be related to the scattering function for a semdilute solution. Consider thermal fluctuations of the local concentration C from its average value of C_b. The free energy associated with these fluctuations $\delta\mathcal{F}$ can be calculated from Eq. (A2) and is found to be

$$\delta\mathcal{F}=\frac{T}{X^3}\int dV\left[\frac{\alpha X^2}{2^{9/20}x_b^{5/4}}(\nabla\delta x)^2+\frac{45}{32}\beta x_b^{1/4}(\delta x)^2\right], \tag{A6}$$

where $x=C/C^*$ and $\delta x=(C-C_b)/C^*$. By taking the Fourier transform of δx, we can rewrite the integral in Eq. (A6) as a sum over Fourier modes δx_q,

$$\delta\mathcal{F}=\frac{T}{X^3}\sum_q|\delta x_q|^2\left(\frac{\alpha X^2}{2^{9/20}x_b^{5/4}}q^2+\frac{45}{32}\beta x_b^{1/4}\right). \tag{A7}$$

For low q values the scattering function $S(q)$ is given in standard notation by (Chap. 13, Sec. 2.6.3 of Ref. 21)

$$S(q)=\frac{S(0)}{1+q^2\xi_e^2}, \tag{A8}$$

where q is the wave vector and ξ_e is the physical screening length of the solution which is related to the screening length ξ by (Chap. 13, Sec. 2.6.3 of Ref. 21)

$$\xi_e=\Gamma\xi, \tag{A9}$$

where Γ is a universal constant.

To determine the scattering function, we invoke the relation $S(q)=\langle|\delta x_q|^2\rangle$, (Chap. 7, Sec. 2 of Ref. 21). By the equipartition theorem, $\langle|\delta x_q|^2\rangle$ is given by

$$\langle|\delta x_q|^2\rangle=\frac{X^3}{2}\left(\frac{\alpha X^2}{2^{9/20}x_b^{5/4}}q^2+\frac{45}{32}\beta x_b^{1/4}\right)^{-1}, \tag{A10}$$

and hence from Eq. (A8), we can see that ξ_e^2 is

$$\xi_e^2=\frac{1}{2^{9/20}}\frac{32}{45}\frac{\alpha}{\beta}\xi^2. \tag{A11}$$

Finally, from Eq. (A9), we can express the ratio α/β in terms of the constant Γ,

$$\frac{\alpha}{\beta}=2^{9/20}\frac{45}{32}\Gamma^2. \tag{A12}$$

Using known experimental and theoretical values for F_∞ and Γ [Eqs. (13.2.35) and (13.2.128) and Chap. 15, Sec. 4.2.4 of Ref. 21] enables the constants α and β to be determined from Eqs. (A5) and (A12). Using theoretical values for F_∞ and Γ, the constants α and β are found to be

$$\alpha\simeq 0.10 \quad \text{and} \quad \beta\simeq 1.97. \tag{A13}$$

APPENDIX B: THE UNIVERSAL POLYMER CONSTANT ρ

In Sec. II B, we formulated, within the scaling framework, the free energy associated with a nonadsorbing polymer solution confined between two parallel planar surfaces. In the limit where the intersurface separation r is much larger than the correlation length ξ of the confined polymer solution, the free energy per unit area can be written as (see Sec. II B)

$$\frac{F}{A}=\frac{\beta T}{a^3}\bar{\phi}^{9/4}r+2\frac{\rho T}{a^2}\bar{\phi}^{3/2}, \tag{B1}$$

where a is a monomeric length scale, $\bar{\phi}$ is the average monomer volume fraction, r is the intersurface separation, and β and ρ are universal constants. In this limit ($r\gg\xi$), the two surfaces can be regarded as independent and thus the first term in Eq. (B1) represents the "bulk" free energy contribution, while the second term represents the free energy per unit area associated with a depletion region near a surface (the factor of 2 arises because we have *two* depletion regions). In this appendix, we determine a value for the constant ρ.

Using the Cahn–de Gennes scaling functional approach,[12,14] we can write the free energy per unit area associated with full depletion of a polymer solution for a single planar surface as

$$\frac{F_{\text{dep}}}{A}=\frac{\beta T}{a^3}\int_0^\infty\left[\frac{\alpha a^2}{\beta\phi^{4/5}(\phi+\bar{\phi})^{9/20}}\left(\frac{d\phi}{dz}\right)^2+\phi^{9/4}-\frac{9}{4}\bar{\phi}^{5/4}\phi+\frac{5}{4}\bar{\phi}^{9/4}\right]dz, \tag{B2}$$

where ϕ is the local monomer volume fraction (the volume fraction of the bulk is just the average volume fraction $\bar{\phi}$), and α and β are the universal polymer constants (see Appendix A). Comparison of the functional expression of Eq. (B2) with the depletion term in the scaling expression of Eq. (B1) then gives the following expression for ρ:

$$\rho=\frac{\beta\bar{\phi}^{-3/2}}{a}\int_0^\infty\left[\frac{\alpha a^2}{\beta\phi^{4/5}(\phi+\bar{\phi})^{9/20}}\left(\frac{d\phi}{dz}\right)^2+\phi^{9/4}-\frac{9}{4}\bar{\phi}^{5/4}\phi+\frac{5}{4}\bar{\phi}^{9/4}\right]dz. \tag{B3}$$

To evaluate this, it is convenient to normalize ϕ by $\bar{\phi}$, introducing $\theta=\phi/\bar{\phi}$, and to measure all lengths in units of the correlation length $\xi=a\sqrt{\alpha/\beta}\bar{\phi}^{-3/4}$, e.g., $z=\xi\tilde{z}$. In the reduced units, we can write Eq. (B3) as

$$\rho=\beta\sqrt{\frac{\alpha}{\beta}}\int_0^\infty\left[\frac{1}{\theta^{4/5}(1+\theta)^{9/20}}\left(\frac{d\theta}{d\tilde{z}}\right)^2+\theta^{9/4}-\frac{9}{4}\theta+\frac{5}{4}\right]d\tilde{z}. \tag{B4}$$

Minimization of the functional expression in Eq. (B4) with respect to changes in the profile gives a Euler–Lagrange equation and boundary condition at the surface

$$\frac{1}{\theta^{4/5}(1+\theta)^{9/20}}\left(\frac{d\theta}{d\tilde{z}}\right)^2=\theta^{9/4}-\frac{9}{4}\theta+\frac{5}{4}, \quad \theta(0)=0. \tag{B5}$$

Solving the profile equations (B5) and then substituting the result into Eq. (B4) enables ρ to be determined.

It is not possible to solve analytically the profile equations (B5) and thus we solve the equations numerically. From the numerically calculated profiles, the value of ρ is then calculated, giving

$$\rho\simeq 2.3\beta\sqrt{\frac{\alpha}{\beta}}. \tag{B6}$$

Finally, substitution of the known value for the ratio α/β [we choose to work with the theoretical estimates (see Appendix A)] gives

$$\rho\simeq 0.5\beta. \tag{B7}$$

[1] P. Kekicheff, B. Cabane, and M. Rawiso, J. Colloid Interface Sci. **102**, 51 (1984).
[2] R. Lipowsky and S. Leibler, Phys. Rev. Lett. **56**, 2541 (1986).
[3] S. Leibler and R. Lipowsky, Phys. Rev. B **35**, 7004 (1987); Phys. Rev. Lett. **58**, 1796 (1987).
[4] S. T. Milner and D. Roux, J. Phys. France I **2**, 1741 (1992).
[5] H. Wennerstrom, Langmuir **6**, 834 (1990).
[6] J. T. Brooks, C. M. Marques, and M. E. Cates, Europhys. Lett. **14**, 713 (1991).
[7] J. T. Brooks, C. M. Marques, and M. E. Cates, J. Phys. France II **1**, 673 (1991).
[8] J. T. Brooks, Ph.D. thesis, Cambridge University, United Kingdom, 1992.
[9] M. Daoud and P.-G. de Gennes, J. Phys. France **38**, 85 (1977).
[10] P.-G. de Gennes, *Scaling Concepts in Polymer Physics* (Cornell University, Ithaca, N.Y., 1979).
[11] P. J. Flory, *Principles of Polymer Chemistry* (Cornell University, Ithaca, N.Y., 1967).
[12] P.-G. de Gennes, Macromolecules **14**, 1637 (1981).
[13] M. E. Cates, D. Roux, D. Andelman, S. T. Milner, and S. A. Safran, Europhys. Lett. **5**, 733 (1988); (Erratum) **7**, 94 (1988).
[14] P.-G. de Gennes, Macromolecules **15**, 492 (1982).
[15] W. Helfrich, Z. Naturforsch. Teil A **33**, 305 (1978).
[16] D. Andelman, M. E. Cates, D. Roux, and S. A. Safran, J. Chem. Phys. **87**, 7229 (1987).

[17] J. N. Israelachvili, *Intermolecular and Surface Forces* (Academic, Orlando, 1985).
[18] R. P. Rand, Annu. Rev. Biophys. Bioeng. **10**, 277 (1981), and references therein.
[19] G. Rossi and P. A. Pincus, Macromolecules **22**, 276 (1989).
[20] J. C. van de Pas and C. J. Buytenhek, Colloids Surf. **68**, 127 (1992).
[21] J. des Cloizeaux and G. Jannink, *Polymers in Solution* (Clarendon, Oxford, 1990).